

Zhanar S. Akhmetkarimova<sup>1,2\*</sup> , Gulshakhar K. Kudaibergen<sup>2</sup> ,  
Guldarigash K. Kaukabaeva<sup>2</sup> , Sailau K. Abeldenov<sup>2</sup> , Aidana B. Rysbek<sup>2</sup> 

<sup>1</sup>University of Reading, Reading, UK

<sup>2</sup>National Center for Biotechnology, Astana, Kazakhstan

(\*Corresponding author's e-mail: [z.akhmetkarimova@reading.ac.uk](mailto:z.akhmetkarimova@reading.ac.uk))

## Thiol-Ene Click Synthesis of Alginate Hydrogels Loaded with Silver Nanoparticles and Cefepime

Hydrogels used in biomedical applications, particularly for soft tissue treatment and regeneration, should have favorable mechanical properties and biocompatibility. Alginate hydrogels are suitable for developing wound dressings with desirable porosity, facilitating effective gas and vapor exchange necessary for wound healing. In this study, we present the synthesis and characterization of photocrosslinked hydrogels based on sodium alginate allyl glycidyl ether (SA-AGE). The composition and structure of the synthesized macromers were confirmed using nuclear magnetic resonance spectroscopy (1H-NMR), while scanning electron microscopy (SEM) revealed the presence of pores ranging in size from 5–32 µm. The UV light polymerization of SA-AGE hydrogel using the photoinitiator I295 was achieved within 60 minutes. The absorption of silver particles and the drug cefepime was determined through titration and UV-spectroscopy, indicating that the optimal concentration was 1 %. The antibacterial activity of the hydrogels loaded with silver nanoparticles and cefepime was evaluated against gram-negative (*Pseudomonas aeruginosa*) and gram-positive (*Staphylococcus aureus*) strains. Cytotoxicity of the hydrogels was assessed using the MTT assay with rat ADMSC cells, and the cell survival rate in the presence of the hydrogels was above 80 %, indicating their non-cytotoxic nature.

**Keywords:** alginate hydrogel, biopolymer, cefepime, photocrosslinked hydrogels, biocompatible, non-toxic, antibacterial activity, tissue engineering.

### Introduction

The significance of wound infection has increased in the past few years, with surgical wounds being particularly affected and often resulting in severe sepsis. The primary contributors to this problem are gram-negative bacteria that have become nearly resistant to all existing antimicrobial drugs. Therefore, the development and implementation of innovative drugs and wound dressings, methods of treatment of purulent and chronic wounds are an urgent task for many researchers [1–3].

To produce an ionic polysaccharide sodium alginate, brown algae is extracted using an alkaline solution. Sodium alginate remains highly valued among naturally derived water-soluble polymers due to its numerous practical benefits. Its ability to form hydrogels in aqueous solutions in the presence of calcium ions has sparked increasing interest among researchers. The hydrogels based on sodium alginate possess remarkable properties such as high-water retention, biodegradability, and non-toxicity, making them ideal for a range of biotechnological, pharmaceutical, and medical applications [4–6]. They are particularly valuable for developing wound healing dressing and drug delivery systems [7]. Sodium alginate is known for its diverse range of biological activities, including antiviral, immunomodulatory, and hemostatic properties [8]. Alginate gels are widely used in the fields of medicine, drug delivery systems, and tissue engineering due to their ease of gelation, affordable cost, biocompatibility, low toxicity, biodegradability, hypoallergenic properties, and chelating ability [3].

Upon reviewing the available literature, our analysis indicated that there have been no previous studies on wound dressings incorporating cefepime, an antibacterial agent from the fourth generation of cephalosporin antibiotics (Fig. 1). It is worth highlighting that cefepime exerts a bactericidal effect by impeding the synthesis of microbial cell walls. Moreover, it demonstrates a wide range of activity against both gram-positive and gram-negative bacteria, including strains that are resistant to third-generation cephalosporin antibiotics and/or aminoglycoside [9].

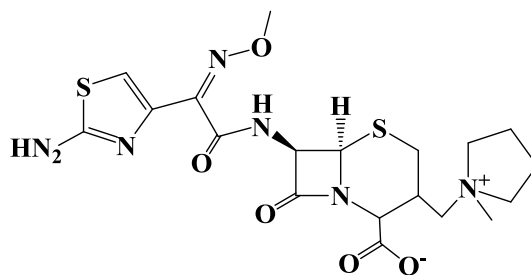


Figure 1. Chemical structure of cefepime

Cefepime demonstrates remarkable resistance to hydrolysis by most beta-lactamases and possesses rapid penetration into the cells of gram-negative bacteria. Its primary molecular target within bacterial cells is the penicillin-binding proteins. Cefepime exhibits efficacy against various gram-positive aerobes, both *in vitro* and *in vivo*, including *Staphylococcus aureus*, *Streptococcus pneumoniae*, *Streptococcus pyogenes*, and *Streptococcus viridans*. It also proves effective against gram-negative microorganisms such as *Proteus mirabilis*, *Pseudomonas aeruginosa*, *Escherichia coli*, *Enterobacter spp.*, and *Klebsiella pneumoniae* [10, 11].

At the same time, ionic silver exhibits bactericidal, strong antifungal, and antiseptic effects, making it a potent disinfectant against pathogenic microorganisms responsible for acute infections. When silver ions are absorbed by the cell membrane of microbes, they disrupt certain cellular functions while keeping the cell viable. This mechanism represents the interaction between silver and microbial cells [11].

To obtain novel derivatives of sodium alginate with specific properties, the click chemistry method, specifically thiol-ene reactions, was used. It is worth highlighting that click chemistry refers to a set of chemical reactions designed for the rapid and reliable synthesis of compounds by seamlessly connecting individual components. Thiol-ene reactions offer notable advantages, such as versatile reaction conditions (including radical reactions and catalytic processes) and the ability to use a wide range of substrates with various unsaturated bonds, such as acrylates, methacrylates, and ethers [12]. Over the past few years, this reaction method has become widely used in different scientific and technological domains, making a significant impact to the development of biomedical materials. Therefore, the click chemistry method, particularly thiol-ene reactions, has emerged as an excellent tool for producing materials with diverse purposes.

Hence, the aim of this study is to employ thiol-ene click synthesis to produce alginate hydrogels loaded with silver nanoparticles and cefepime, and to investigate their chemical and biological properties. Specifically, the purposes include determining the NMR structure of alginate macromers, assessing the sol-gel fraction and degradation extent of the alginate hydrogel, evaluating the antibacterial activity of the hydrogel impregnated with silver particles and cefepime using disk diffusion tests against *Pseudomonas aeruginosa* and *Staphylococcus aureus*, and lastly, examining the cytotoxicity of the hydrogel through MTT assay on the viability of rat ADMSC cells.

## Experimental

### Preparation and characterization of hydrogel

The synthesis of sodium alginate (SA) and allyl glycidyl ether (AGE) was performed based on a previously reported method [13], with some modifications. Briefly, a 2 % (w/v) solution of SA was prepared by mixing 10 mL of Milli-Q water. Continuous stirring was employed while adding 0.96 g of AGE to the alginate solution. Concentrated acetic acid was added to adjust the pH to 3. The reaction was carried out at 60 °C for six hours. A generous amount of cold ethanol was added to precipitate the solution. The product was then subjected to 2–3 ethanol washes and subsequently freeze-dried. The entire synthesis process of sodium alginate allyl glycidyl ether (SA-AGE) was carried out in complete darkness.

Assessment of hydrogel density, gel fractions, and degradation degree involved the use of established methods. These measurements were performed to determine the gel yield, employing a well-established equation [14]:

$$\text{Gel}(\%) = \frac{W_w}{W_i} \times 100, \quad (1)$$

where  $W_w$  and  $W_i$  — the weights of the dry and swollen samples respectively.

Following that, the hydrogels labeled as  $W_1$  were weighed and transferred into sterile PBS tubes (0.1 M, pH 7.4) with a volume of 50 ml. During the 8-week incubation period at 37 °C, the solution was changed twice a week. At specific intervals, hydrogel samples were removed from the solution and rinsed with deionized water. After subjecting the samples to 24 hours of freeze-drying (resulting in samples labeled as  $W_2$ ), the degree of degradation was determined using the subsequent equation [14, 15]:

$$DD(\%) = \frac{W_1 - W_2}{W_1} \times 100. \quad (2)$$

The gravimetric method was used to study the swelling process. The mass degree of swelling, represented as a percentage, was determined by comparing the mass of the swollen structured hydrogel to its initial mass. This equation was utilized to quantify the intensity of swelling:

$$\alpha(\%) = \frac{m_n - m_1}{m_1} \times 100, \quad (3)$$

where  $m_1$  — the mass of the sample before the start of the study, g;  $m_n$  — the mass of the sample after a certain time, g.

Separately, concentration of 2.5 % (w/v) of SA-AGE was achieved in borosilicate vials by dissolving it in Milli-Q water. In respect of the macromer, I295 was added to the resulting solution (w/v) at different concentrations (2.5 %, 5 %, and 10 %, respectively), and UV light (365 nm) was then applied for 1 hour.

The <sup>1</sup>H NMR spectra of the samples were recorded on a JNM-ECA 500 spectrometer (JEOL, USA) operating at a central field strength of 11.74 (500 MHz <sup>1</sup>H), with a current below 95 Amps and field stability (drift) of less than 5 Hz/hr <sup>1</sup>H drift. The inductance of the spectrometer was 146 H (nominal). MestreNova software was employed to process the spectral data. All samples were dissolved in D<sub>2</sub>O at a concentration of 1 % (w/v) to obtain the spectra. The extent of MA substitution in the GG backbone was evaluated by analyzing the <sup>1</sup>H NMR spectra. The percentage degree of MA substitution (%DM) in the GG chain was determined using the following equation [14]:

$$\%DM = \frac{H_b + H_c / 2}{GG - 1 / 6} \times 100, \quad (4)$$

where  $H_c$ ,  $H_b$  and  $GG - 1$  — the signals of the anomeric carbon hydrogen in the mannuronic units (ca. 3.70–3.90 ppm), the relayed peaks of the anomeric carbon hydrogen, and in the methacrylate group the two vinyl hydrogens (5.00–5.75 ppm), respectively.

The method is based on the formation of a yellow-colored silver-dithizone complex and subsequent extraction of the silver-dithizone complex into a layer of tetrachloroethylene at pH 1.5–2.0. Colorimetry is performed using the method of standard series based on mixed-color formation [16]. 20 ml of the test solution containing 0.1–1 N sulfuric acid is placed into a separating funnel and diluted with water to a total volume of 50 ml. The mixture is titrated with a dithizone solution until the silver is completely extracted, which means that the extract, after 30 seconds of shaking, retains a green instead of the initial golden-yellow color. The accuracy of this method of determination is 0.5 %.

Cefepime was incorporated into the alginate hydrogel loaded silver nanoparticles using the absorption method. The degree of cefepime absorption was analyzed using spectrophotometry in the short-wave region. The optical density of standard and adsorbed solutions was measured using an “Eco-chem” scanning spectrophotometer, model PE-5300VI. A mixture of dimethyl sulfoxide and water (5:5) was used as a reference solution in quartz cuvettes with a 10 mm working layer thickness at a wavelength of 265 nm. The procedure for constructing a calibration curve for the analyzed substances was as follows: 0.01, 0.03, 0.05, 0.07, 0.09, 0.15, and 0.18 mL of the analyzed substance solution in water (1 mg/mL) were added into 10 mL volumetric flasks. 4.99, 4.97, 4.95, 4.93, 4.85, and 4.82 mL of water, respectively, were added to each flask. Then, 5 mL of dimethyl sulfoxide were added to each flask. The quantitative value of the adsorbed drug was determined using the calibration curve, taking into account the sample of the taken drug.

The antibacterial properties of alginate hydrogel samples were evaluated by the microbiological disc diffusion method, namely, the measurement of growth inhibition zones of test cultures *Staphylococcus aureus* and *Pseudomonas aeruginosa*. For the study, bacterial cultures of *Staphylococcus aureus* with a titer of  $9.1 \times 10^{10}$  CFU/ml and *Pseudomonas aeruginosa*  $6 \times 10^7$  CFU/ml were selected after incubation for 14 hours in a liquid nutrient broth on a shaker at 150 rpm and temperature 37 °C. Samples of hydrogels containing particles of silver and antibiotic cefepime (in various concentrations) were placed on LB agar medium no later than 15 minutes after inoculation with sterile cotton swabs, streaking a suspension (culture fluid)

of a certain density equivalent to a turbidity standard of 0.5 according to McFarland and incubated at 37 °C. The hydrogel was pre-sterilized with a UV lamp for 15 minutes (254 nm). To compare the antibacterial activity of different samples of hydrogels containing different concentrations of silver and/or cefepime particles, the diameters of the growth inhibition zones of test cultures in millimeters were measured relative to the size of the hydrogel discs.

The dried hydrogels were examined for their morphology using a scanning electron microscope (SEM, Auriga Crossbeam 540, Carl Zeiss) operating in SE2 signal mode. The SEM was configured with an analytic column, a working distance (WD) of 4.6 mm, noise reduction Line Int. Busy SB Grid 833 V, and a scan speed of 3.

The cells were cultured at different densities ( $1-5 \times 10^6$  cells per mL) in a transparent plate following the desired protocol. In the case of suspension cells, the 96-well plates were centrifuged at  $1,000 \times g$ , 4 °C for 5 minutes using a microplate-compatible centrifuge, and the media was carefully removed. Then, 50  $\mu$ L of serum-free media and 50  $\mu$ L of MTT Reagent were added to each well. For the background control wells, 50  $\mu$ L of MTT Reagent and 50  $\mu$ L of cell culture media (without cells) were prepared. The plate was incubated at 37 °C for 3 hours. After incubation, 150  $\mu$ L of MTT solvent was added to each well. The plate was covered with foil, placed on an orbital shaker, and shaken for 15 minutes. The absorbance was measured at OD = 590 nm. The study was carried out according to the guidelines of the Declaration of Helsinki and approved by the Local Ethics Committee of the National Center for Biotechnology [17].

For the statistical analysis, all the physical, chemical, and biological experiments on hydrogel samples were performed in triplicate. All the experimental values were expressed in the form of mean  $\pm$  standard error and the limit of experimental error of each test was  $\pm 5\%$ , which had been considered as statistically significant.

### Results and Discussion

The preparation of SA-AGE hydrogel generally involved a reaction at pH 3 and 60 °C for 6 hours. It is worth noting that allyl glycidyl ether is a saturated three-membered heterocycle with a single oxygen atom in the cycle. Epoxides exhibit a redistribution of electron density from carbon atoms to oxygen atoms, resulting in a high level of strain within the three-membered cycle. These characteristics significantly affect their reactivity. For instance, in a neutral or basic medium, the reaction proceeds under kinetic control, and the nucleophile attacks the carbon atom with the least steric hindrance in the substrate.

The reaction between sodium alginate and allyl glycidyl ether was carried out at a pH value of 3. During the reaction, there was a significant redistribution of electron density when the epoxy ring opened. As a result, the nucleophile interacts with the substrate at the carbon atom with the highest substitution, where the majority of the positive charge is concentrated. Consequently, the SA-AGE macromer is formed as a product of epoxy ring opening under acidic conditions. These conditions are characterized by the influence of thermodynamic control on the direction of the processes (Fig. 2).

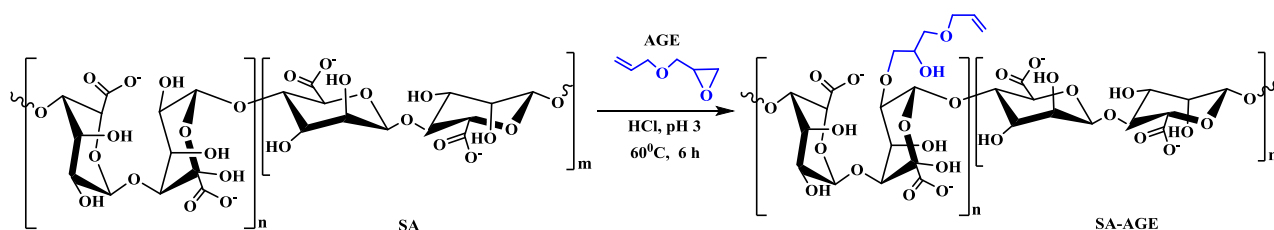


Figure 2. Reaction scheme of the SA-AGE macromer

The analysis of the  $^1\text{H}$  NMR spectrum of the SA-AGE macromer revealed that the signals of the protons of the CH-, CH<sub>2</sub>- groups of the glucose part of the molecule appear in the region of 3.24–3.57 ppm. in the form of a complex multiplet. The anomeric proton H(1) of the carbohydrate residue appears as a doublet at 3.72 ppm. (d,  $J=3.9$  Hz, 9H), characteristic of the  $\beta$ -anomer and indicating the interaction of the anomeric proton only with the neighboring trans-axial proton at C2. The methylene protons of the vinyl fragment CH=CH<sub>2</sub> appear as a multiplet in the region of 5.30–5.00 ppm (=CHa). The signal at 5.79 ppm. in the form of a singlet, corresponds to the vinyl protons of the epoxide. The methine proton of the OCH= fragment is written as a singlet at 1.02 ppm. The integral curve corresponds to the total number of protons (Fig. 3).

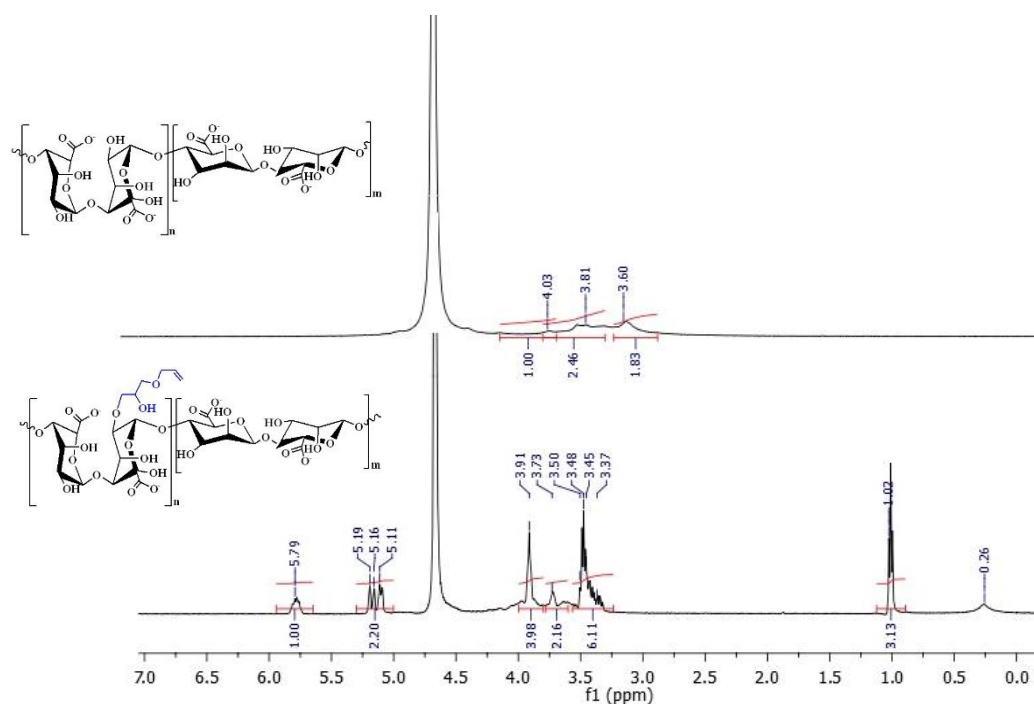


Figure 3. NMR spectra of the SA-AGE macromer

The SA-AGE structure includes a sugar group and an unsaturated double bond, making it a versatile building block for the synthesis of various medicinal copolymers. These copolymers not only exhibit prolonged release properties but also enable targeted drug delivery to specific cells in the body that possess carbohydrate-binding proteins on their surfaces (Fig. 4).



Figure 4. Scheme formation of composite hydrogel dressing with drug delivery

In order to control the speed and effectiveness of UV activation, we employed the sol-gel analysis technique, which enables the quantification of insoluble (spatially cross-linked) and soluble polymers. Following UV activation, samples with varying ratios of the thiol derivative (S-H bond) exhibited low viscosity, indicating the predominant degradation of polymer molecules in these systems. The dominant process in allyl-alginate molecules is the breaking of bonds rather than their formation, as alginate polymer derivatives primarily exhibit a deconstructing behavior. The amount of gel fraction reflects the effectiveness of polymer cross-linking, which in turn influences the immobilization efficiency of the medicine in the hydrogel matrix and its release rate. As depicted in Figure 5a, the yield of the gel fraction is significantly higher for the SA-AGE-100 sample compared to the SA-AGE-50. This difference can be attributed to the higher molecular weight polymer and its impact on the degree of cross-linking, rather than polymer modification. Unfortunately, the SA-AGE-25 sample was dissolved in Milli-Q and did not participate in subsequent experiments.

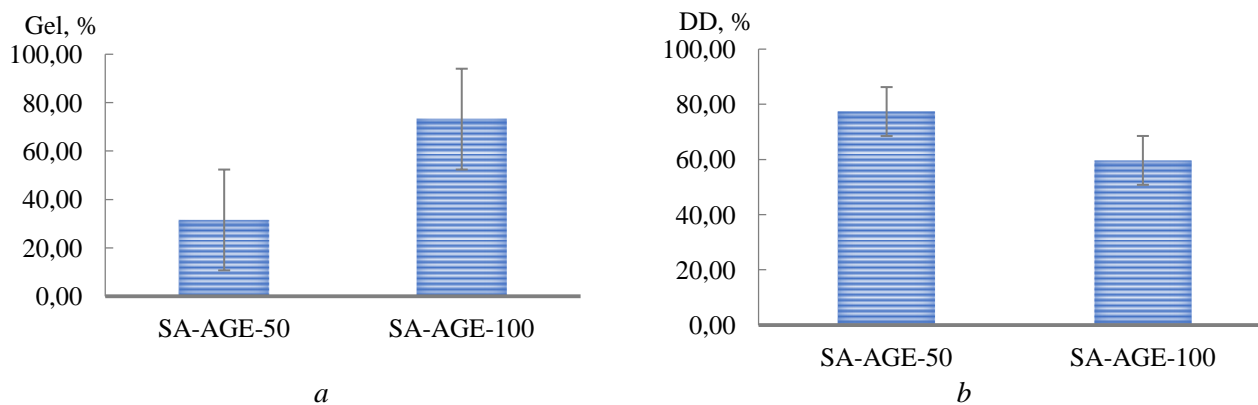


Figure 5. General properties of the SA-AGE macromer: (a) sol-gel, (b) degradation degree

As for degradation, it involves the hydrolysis process that breaks down the walls of cryogel macropores, resulting in mass loss. The study of SA-AGE-50 and SA-AGE-100 hydrogel degradation at 37 °C, over time showed a weight loss (Fig. 5b). Within 8 weeks,  $77.35 \pm 1.1\%$  and  $59.64 \pm 1.4\%$  degraded, respectively. It was noted that the hydrogel with a lower concentration exhibited a higher degree of degradation due to the density of crosslinking and the hydrophilic properties of the polymers. Based on the obtained data, it can be concluded that hydrogels demonstrate a low level of degradation and can be further used as scaffolds for drug delivery.

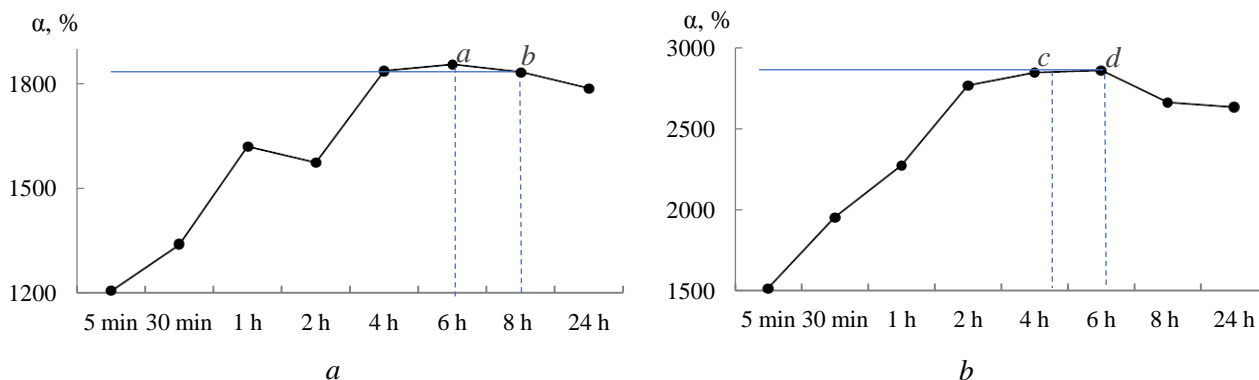


Figure 6. Sample swelling kinetic curve SA-AGE-100 (a) and SA-AGE-50 (b)

Figure 6 illustrates the continuous increase in swelling when the SA-AGE-50 and SA-AGE-100 samples are immersed in the liquid. After 6 hours (point a) and 4 hours (point c), the swelling rate starts to decrease, indicating a gradual slowdown in swelling over time and reaching the maximum possible swelling due to the initial intense swelling. At points a and c, the dissolution rate becomes equal to the swelling rate, resulting in a constant degree of swelling. After 8 hours (point b) and 6 hours (point d), the dissolution rate begins to exceed the swelling rate, leading to a decrease in the weight of the samples. It was determined that between points a and b, as well as c and d, the samples exhibit maximum swelling.

In conclusion, the experimental data obtained suggest that SA-AGE-100 exhibits a higher efficiency of crosslinking. Therefore, this specific sample was selected as the focus for further investigation of its antibacterial and toxicological activity.

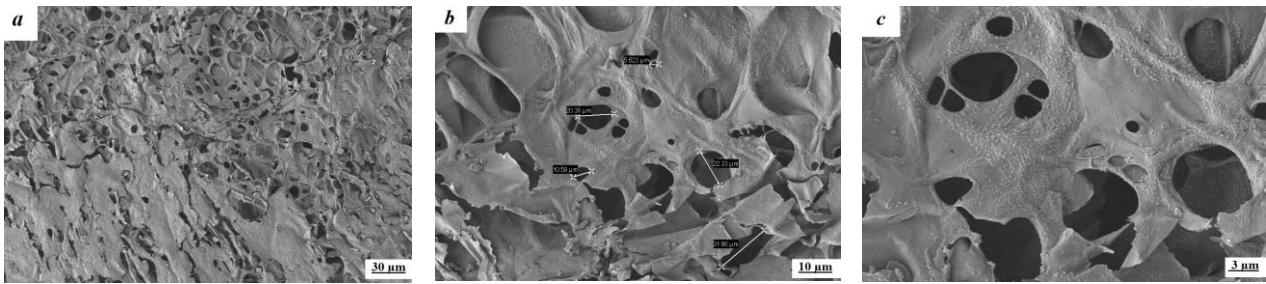


Figure 7. SEM of SA-AGE-100 hydrogel

The SEM micrographs of SA-AGE-100 showed a uniform cross-sectional morphology of the samples, which confirms the good miscibility and homogeneity between the ingredients of the composite hydrogels. The synthesized hydrogel forms a hetero-porous (with interconnected pores) polymer matrix structure in which macromolecules are connected into a stable 3D network (Fig. 7a). However, there are differences in morphology, in particular in the size and regularity of their arrangement (Fig. 7b, 7c). The electron micrograph shows differences in the porosity of the structure; there are both micropores with a dimension of 6  $\mu\text{m}$  and macropores up to 32  $\mu\text{m}$ . The resulting pore sizes are appropriate for drug delivery given that accommodates more silver particles and cefepime molecules, whereupon agglomerating. Thus, the pores allow for cell-cell communication with silver particles and cefepime and are available as a medical device in regenerative medicine.

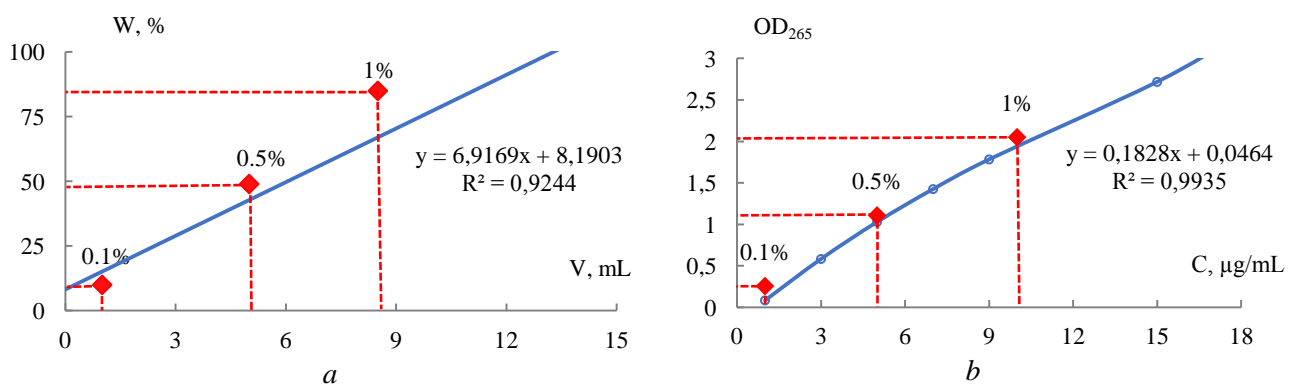


Figure 8. Quantitative analysis of the silver particles (a) and cefepime (b)

The concentration of silver and cefepime particles was quantitatively determined through photometric titration, generating the relationships between solution optical density and their respective concentrations (Fig. 8). The absorption dynamics of the antibacterial agents introduced into the samples was studied under static conditions, focusing on the volume comparison.

The intensity of absorption was assessed by measuring it at a specific wavelength, using concentration-dependent curves of the absorption intensity for silver and cefepime particles (Fig. 7a) as references. The analysis revealed an absorption degree of 85 % for silver particles (Fig. 8a) and a concentration of 10  $\mu\text{g/mL}$  for cefepime (Fig. 8b). Overall, these findings indicate that the optimal concentration of impregnated silver and cefepime particles within the SA-AGE hydrogel structure was determined to be 1 % [18].

An essential requirement for a wound-healing dressing is its non-toxic nature. Therefore, the toxicity of SA-AGE-50 and SA-AGE-100 hydrogels on rat ADMSC cells was evaluated using the MTT assay (Fig. 9). The percentage of cell survival was determined by calculating the ratio of the spectral absorbance ( $\text{OD}_{\text{exp}}$ ) in the experimental group to the spectral absorbance ( $\text{OD}_{\text{contr}}$ ) in the control group.

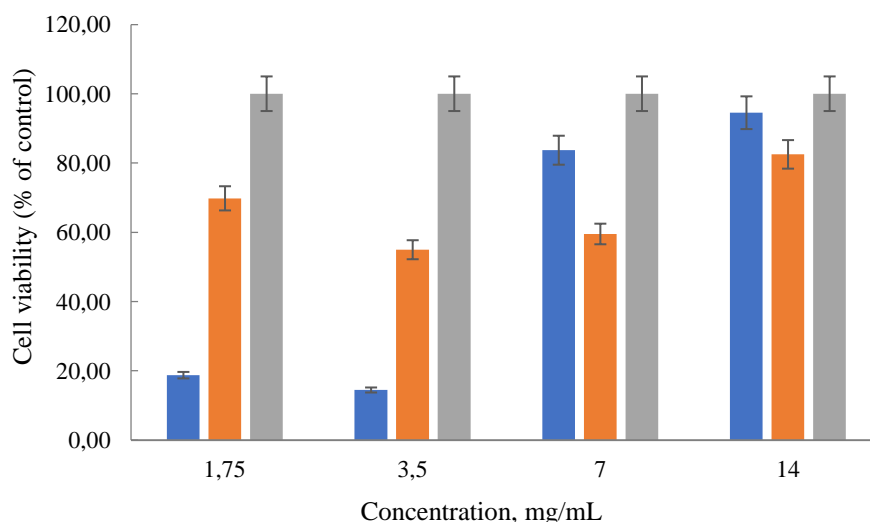


Figure 9. Cytotoxicity of SA-AGE-50 and SA-AGE-100 hydrogels to rat ADMSC cells by MTT assay

According to the international standard ISO 10993–5:2009(E), cytotoxicity is divided into six grades i.e., 0, 1, 2, 3, 4, and 5, which corresponds to 100 %, 75 %-99 %, 50 %-74 %, 25 %-49 %, 1 %-24 %, and 0 in the percentage of cell survival respectively, and grades 0 and 1 are considered non-cytotoxicity [19]. The cell survival percentage of these two hydrogels was above 80 %, indicating the absence of cytotoxicity.

Table

#### Antibacterial activity of SA-AGE-100

Strains /samples	A 0.1 %	C 0.1 %	A 0.5 %	C 0.5 %	C 1 %	A 1 %	A-C 1 %
<i>P. aeruginosa</i>	5.3±0.4	10.3±1.8	3.3±0.4	11.7±0.4	12.3±0.4	4.3±0.4	12.0±0.7
<i>S. aureus</i>	2.0	10.3±1.6	2.0	9.0±1.3	10.7±0.4	2.7±0.4	8.7±1.1

The antimicrobial efficacy of SA-AGE-100, incorporating silver particles and cefepime, was assessed against one gram-negative strain of *Pseudomonas aeruginosa* and one gram-positive strain of *Staphylococcus aureus*. These specific strains were chosen to represent different bacterial mechanisms that possess multiple virulence factors, as well as their pathogenicity and prevalence in everyday life. Various ratios of wound dressings were prepared for the study, containing different concentrations (0.1 %, 0.5 %, and 1 %) of silver particles (A) and cefepime (C) absorbed within the alginate coating structure. Additionally, a mixture of A-C at a concentration of 1 % was also included in the research.

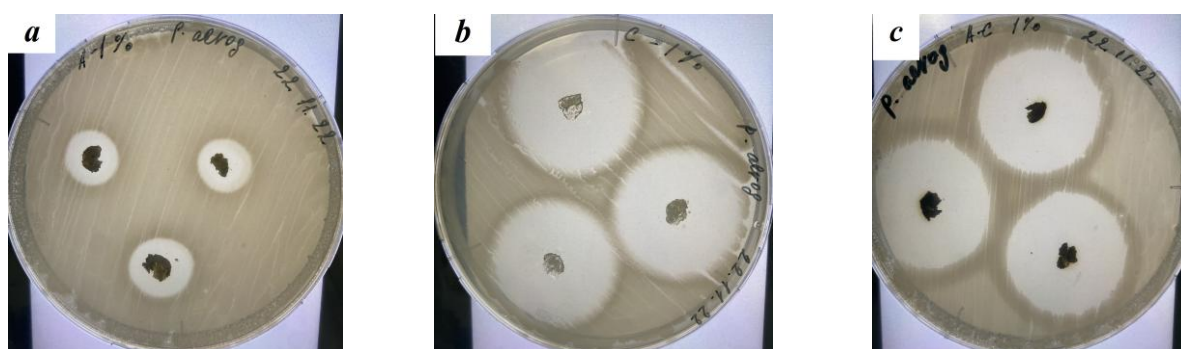


Figure 10. Evaluation of antibacterial activity of SA-AGE-100 loaded with: (a) silver particles 1 %; (b) cefepime 1 %; (c) mixture of silver particles 1 % and cefepime 1 %.

The study demonstrated the inhibitory effect of silver particles and cefepime on bacterial growth upon diffusion into agar (Table). Interestingly, both the mixture of silver particles and cefepime and pure cefepime

exhibited similar zones of inhibition (Fig. 10b, 10c), while the silver particles alone showed a more moderate outcome (Fig. 10a).

Based on our initial findings, it is evident that the adsorbed silver particles and cefepime in the alginate matrix exhibit a strong antibacterial activity. Specifically, samples C-1 and AC-1 demonstrate promising results and are therefore recommended for further investigation [20].

### Conclusions

This study presents an experimental characterization of photocrosslinked SA-AGE hydrogels, aiming to evaluate and explain their physicochemical and biological properties. The obtained kinetic parameters of the swelling-dissolution process indicate that the synthesized SA-AGE hydrogel is capable of providing a diffusion prolonged release of drugs. Furthermore, when loaded with silver particles and cefepime, the synthesized hydrogel effectively delivers these substances to the tested bacterial strains, demonstrating high antibacterial activity without toxicity. However, further *in vivo* studies are necessary to assess the fate and toxicity of SA-AGE-100 before definitive conclusions can be drawn regarding the utility of the synthesized drugs. These preliminary results can serve as foundational data for the development of medical products.

### Acknowledgments

The Committee of Science of the Ministry of Science and Higher Education of the Republic of Kazakhstan provided financial support for this study (Grant No. AP13068136). All measurements were performed using equipment of the Nazarbayev University.

The authors express their gratitude to Amantay Nazerke and Amantay Fatima for their contribution in designing all the images.

### References

- 1 Vigata, M., Meinert, C., Hutmacher, D. W., & Bock, N. (2020). Hydrogels as drug delivery systems: A review of current characterization and evaluation techniques. *Pharmaceutics*, *12*(12), 1188. <https://doi.org/10.3390/pharmaceutics12121188>
- 2 Ogay, V., Mun, E. A., Kudaibergen, G., Baidarbekov, M., Kassymbek, K., Zharkinbekov, Z., & Saparov, A. (2020). Progress and prospects of polymer-based drug delivery systems for bone tissue regeneration. *Polymers*, *12*(12), 2881. <https://doi.org/10.3390/polym12122881>
- 3 Qu, J., Zhao, X., Liang, Y., Xu, Y., Ma, P. X., & Guo, B. (2019). Degradable conductive injectable hydrogels as novel antibacterial, anti-oxidant wound dressings for wound healing. *Chemical Engineering Journal*, *362*, 548–560. <https://doi.org/10.1016/j.cej.2019.01.028>
- 4 Shi, Q., Luo, X., Huang, Z., Midgley, A. C., Wang, B., Liu, R., ... & Wang, K. (2019). Cobalt-mediated multi-functional dressings promote bacteria-infected wound healing. *Acta Biomaterialia*, *86*, 465–479. <https://doi.org/10.1016/j.actbio.2018.12.048>
- 5 Aderibigbe, B.A., & Buyana, B. (2018). Alginate in wound dressings. *Pharmaceutics*, *10*(2), 42. <https://doi.org/10.3390/pharmaceutics10020042>
- 6 Chen, K., Wang, F., Liu, S., Wu, X., Xu, L., & Zhang, D. (2020). In situ reduction of silver nanoparticles by sodium alginate to obtain silver-loaded composite wound dressing with enhanced mechanical and antimicrobial property. *International Journal of Biological Macromolecules*, *148*, 501–509. <https://doi.org/10.1016/j.ijbiomac.2020.01.15>
- 7 Diniz, F. R., Maia, R. C. A., de Andrade, L. R. M., Andrade, L. N., Vinicius Chaud, M., da Silva, C. F., ... & Severino, P. (2020). Silver nanoparticles-composing alginate/gelatine hydrogel improves wound healing in vivo. *Nanomaterials*, *10*(2), 390. <https://doi.org/10.3390/nano10020390>
- 8 Lin, X., Guan, X., Wu, Y., Zhuang, S., Wu, Y., Du, L., ... & Tu, M. (2020). An alginate/poly (N-isopropylacrylamide)-based composite hydrogel dressing with stepwise delivery of drug and growth factor for wound repair. *Materials Science and Engineering: C*, *115*, 111123. <https://doi.org/10.1016/j.msec.2020.111123>
- 9 Farhadian, N., Karimi, M., & Porozan, S. (2021). Ceftriaxone sodium loaded onto polymer-lipid hybrid nanoparticles enhances antibacterial effect on gram-negative and gram-positive bacteria: Effects of lipid-polymer ratio on particles size, characteristics, in vitro drug release and antibacterial drug efficacy. *Journal of Drug Delivery Science and Technology*, *63*, 102457. <https://doi.org/10.1016/j.jddst.2021.102457>
- 10 Alshammari, F., Alshammari, B., Moin, A., Alamri, A., Al Hagbani, T., Alobaida, A., ... & Rizvi, S. M. D. (2021). Ceftriaxone mediated synthesized gold nanoparticles: a nano-therapeutic tool to target bacterial resistance. *Pharmaceutics*, *13*(11), 1896. <https://doi.org/10.3390/pharmaceutics13111896>
- 11 Zhang, M., & Zhao, X. (2020). Alginate hydrogel dressings for advanced wound management. *International Journal of Biological Macromolecules*, *162*, 1414–1428. <https://doi.org/10.1016/j.ijbiomac.2020.07.311>
- 12 Kazybayeva, D. S., Irmukhametova, G. S., & Khutoryanskiy, V. V. (2022). Thiol-ene “click reactions” as a promising approach to polymer materials. *Polymer Science, Series B*, *64*(1), 1–16. <https://doi.org/10.1134/S1560090422010055>

- 13 Araiza-Verduzco, F., Rodríguez-Velázquez, E., Cruz, H., Rivero, I. A., Acosta-Martínez, D. R., Pina-Luis, G., & Alatorre-Meda, M. (2020). Photocrosslinked alginate-methacrylate hydrogels with modulable mechanical properties: Effect of the molecular conformation and electron density of the methacrylate reactive group. *Materials*, 13(3), 534. <https://doi.org/10.3390/ma13030534>
- 14 Kudaibergen, G., Zhunussova, M., Mun, E. A., Arinova, A., & Ogay, V. (2021). Studying the Effect of Chondroitin Sulfate on the Physicochemical Properties of Novel Gelatin/Chitosan Biopolymer-Based Cryogels. *Applied Sciences*, 11(21), 10056. <https://doi.org/10.3390/app112110056>
- 15 Kudaibergen, G. K., & Zhunussova, M. S. (2022). Study of the effect of temperature on the properties of gelatin-chitosan cryogels. *Bulletin of the University of Karaganda — Chemistry*, 106(2), 4-11. <https://doi.org/10.31489/2022Ch2/2-22-4>
- 16 Voda pitevaia. Metody opredeleniia sodержaniia svintsia, tsinka, serebra [Drinking water. Methods for determination of lead, zinc and silver content] (1972) *GOST 18293-72 from 25<sup>th</sup> December, 1972*. Moscow: Mezhsudarstvennyi standart [in Russian]. Retrieved from [https://online.zakon.kz/Document/?doc\\_id=31126624&pos=1;-16#pos=1;-16](https://online.zakon.kz/Document/?doc_id=31126624&pos=1;-16#pos=1;-16)
- 17 WMA Declaration of Helsinki — Ethical Principles for Medical Research Involving Human Subjects (2021) Meeting of the Local Ethical Commission of the National Center for Biotechnology Company, Nur-Sultan. Protocol No.4, December 3, 2021.
- 18 Shoaibi, Z. A., & Gouda, A. A. (2012). Extractive spectrophotometric method for the determination of tropicamide. *Journal of Young Pharmacists*, 4(1), 42-48. <https://doi.org/10.4103/0975-1483.93572>
- 19 Chen, Y. M., Xi, T., Zheng, Y., Guo, T., Hou, J., Wan, Y., & Gao, C. (2009). In vitro cytotoxicity of bacterial cellulose scaffolds used for tissue-engineered bone. *Journal of bioactive and compatible polymers*, 24(1\_suppl), 137-145. <https://doi.org/10.1177/0883911509102710>
- 20 Alhakamy, N. A., Caruso, G., Eid, B. G., Fahmy, U. A., Ahmed, O. A., Abdel-Naim, A. B.,... & Abdulaal, W. H. (2021). Ceftriaxone and melittin synergistically promote wound healing in diabetic rats. *Pharmaceutics*, 13(10), 1622. <https://doi.org/doi.org/10.3390/pharmaceutics13101622>

#### Information about the authors\*

**Akhmetkarimova, Zhanar Samatovna** (*corresponding author*) — PhD, Postdoctoral Research Associate (PDRA) in Pharmacy, University of Reading, RG6 6AH, Reading, Berkshire, United Kingdom; Senior researcher, National Center for Biotechnology, Korgalzhin broad, 13/5, 010000, Astana, Kazakhstan; e-mail: [z.akhmetkarimova@reading.ac.uk](mailto:z.akhmetkarimova@reading.ac.uk); <https://orcid.org/0000-0002-9782-5521>;

**Kudaibergen, Gulshakhar Kudaibergenovna** — PhD, Senior researcher, National Center for Biotechnology, Korgalzhin broad, 13/5, 010000, Astana, Kazakhstan; e-mail: [kudaibergen@biocenter.kz](mailto:kudaibergen@biocenter.kz); <https://orcid.org/0000-0002-0779-4099>;

**Kaukabaeva, Guldarigash Kuanyshevna** — Junior researcher, National Center for Biotechnology, Korgalzhin broad, 13/5, 010000, Astana, Kazakhstan; e-mail: [guldarigash.kaukabaeva@mail.ru](mailto:guldarigash.kaukabaeva@mail.ru); <https://orcid.org/0000-0002-9052-5091>;

**Abeldenov, Sailau Kasenovich** — Head of laboratory, National Center for Biotechnology, Korgalzhin broad, 13/5, 010000, Astana, Kazakhstan; e-mail: [abeldenov@biocenter.kz](mailto:abeldenov@biocenter.kz); <https://orcid.org/0000-0002-6974-9138>;

**Rysbek, Aidana Begalykyzy** — 3<sup>rd</sup> year PhD student, Junior researcher, National Center for Biotechnology, Korgalzhin broad, 13/5, 010000, Astana, Kazakhstan; e-mail: [aidanarysbek93@gmail.com](mailto:aidanarysbek93@gmail.com); <https://orcid.org/0000-0001-8290-0552>

\*The author's name is presented in the order: *Last Name, First and Middle Names*